Experimental Neurology 334 (2020) 113458

Contents lists available at ScienceDirect

Experimental Neurology

journal homepage: www.elsevier.com/locate/yexnr

Research paper

The relevance of multimodal assessment in experimental oxaliplatin-induced peripheral neurotoxicity

Eleonora Pozzi[a], Giulia Fumagalli[a], Alessia Chiorazzi[a], Annalisa Canta[a], Cristina Meregalli[a], Laura Monza[a], Valentina Alda Carozzi[a], Norberto Oggioni[a], Virginia Rodriguez-Menendez[a], Guido Cavaletti[a,*], Paola Marmiroli[a,b]

[a] Experimental Neurology Unit, School of Medicine and Surgery, University of Milano-Bicocca, Monza, Italy
[b] Department of Biotechnology and Biosciences, University of Milano-Bicocca, Milano, Italy

ARTICLE INFO

Keywords:
Oxaliplatin neurotoxicity
Mouse models
Multimodal assessment
Mechanical sensitivity
Cold sensitivity
Neurophysiology
Histopathology

ABSTRACT

Chemotherapy-induced peripheral neurotoxicity represents one of the most relevant dose-limiting side effects that can affect cancer patients treated with the common antineoplastic agents. Since the severity of neurotoxicity often leads to dose reduction or early cessation of chemotherapy, the investigation of molecular mechanisms underlying chemotherapy-induced peripheral neurotoxicity is an urgent clinical need in order to better understand its physiopathology and find effective strategies for neuroprotection. Several in vivo preclinical models of chemotherapy-induced peripheral neurotoxicity have been developed but a great variability in mouse strain, dose, route of administration of the drug, treatment schedule and assessment of neurotoxicity is observed between the different published studies making difficult the comparison and interpretation of their results. In many of these studies only behavioural tests are used as outcome measures, while possible neurophysiological and neuropathological changes are not evaluated.

In this study, focused on experimental oxaliplatin-induced peripheral neurotoxicity, we reproduced and compared four mouse models with very different drug dose (low or high dose-intensity) and treatment schedules (short or long-term treatment), selected from the literature. Using a multimodal assessment based on behavioural, neurophysiological and neuropathological methods, we evidenced remarkable differences in the results obtained in the selected animal models. This work suggests the importance of a multimodal approach including extensive pathological investigation to confirm the behavioural results.

1. Introduction

Peripheral neurotoxicity is one of the most relevant, disabling and dose-limiting side effects of cancer treatment. Chemotherapy-induced peripheral neurotoxicity (CIPN) may develop in cancer patients treated with antineoplastic agents like taxanes, vinca alkaloids, proteasome inhibitors, epothilones and platinum compounds (cisplatin, oxaliplatin, carboplatin) (Vilholm et al., 2014).

CIPN is most often characterized by dysesthesias, paresthesias, numbness and sensory loss with a distal and symmetric distribution ("stocking and glove" pattern), that may be accompanied by neuropathic pain and less frequently by motor and/or autonomic impairment. The typical course of CIPN is subacute and progressive, with the exception of paclitaxel and oxaliplatin (OHP) that can also cause an acute and transient neurotoxicity (Marmiroli et al., 2017b).

Since the severity of neurotoxicity often leads to anticancer treatment dose reduction or interruption and there is not approved therapy for its prevention, the investigation of molecular mechanisms underlying CIPN is an urgent need in order to better understand its physiopathology and find possible neuroprotective strategies. For this purpose, several in vivo preclinical models of CIPN have been developed. However, a great variability is observed between the different published studies making difficult the comparison and interpretation of their results. In fact, CIPN rodent models reported in literature differ in species and strain, dose and route of administration of the chemotherapeutic agent, schedule of treatment as well as in the type and/or sensibility of evaluation methods used to assess the onset of neurotoxicity (Bruna et al., 2020; Calls et al., 2020; Gadgil et al., 2019; Marmiroli et al., 2017b). Moreover, several of the reported animal models of CIPN are far from reproducing the typical clinical use of the tested drugs. Most of them consist of single/few administrations or achieve extremely high dose-intensity over a short period of time, as

* Corresponding author at: School di Medicine and Surgery, Via Cadore 48, I-20900 Monza, MB, Italy.
E-mail address: guido.cavaletti@unimib.it (G. Cavaletti).

https://doi.org/10.1016/j.expneurol.2020.113458
Received 10 July 2020; Received in revised form 25 August 2020; Accepted 30 August 2020
Available online 02 September 2020

opposite to a clinical used in which the patients are treated with repeated doses for several weeks/months. In addition, although the common neurotoxic antineoplastic drugs are administered intravenously in cancer patients, the majority of CIPN rodent models are established using the intraperitoneal route of administration (Bruna et al., 2020; Marmiroli et al., 2017b). Therefore, it cannot be excluded that these experimental paradigms might not be optimal for reproducing the full spectrum of chronic CIPN, although they could be effective in inducing neuropathic pain. This observation is related to another critical aspect, represented by the assessment of the CIPN features. In fact, many animal models use only behavioural tests as outcome measures, whereas a multimodal analysis that combines behavioural tests, neurophysiological and histopathological studies could clearly demonstrate the occurrence of CIPN and describe its characteristics, thus allowing a reliable comparison with the clinical feature of chronic CIPN (Gadgil et al., 2019).

To better elucidate these critical points, we performed this study using OHP-induced peripheral neurotoxicity (OIPN) as the selected experimental paradigm to make a comparison among different mouse models. Among the several rodent OIPN models reported in literature, we selected four models with very different drug dose (low or high dose-intensity) and treatment schedules (short or long-term treatment) (Calls et al., 2020; Gadgil et al., 2019).

Each group of treatment was studied with a multimodal toolkit comparing treated animals and their matched controls. Behavioural, neurophysiological and histopathological studies were performed at similar time points in each model until two weeks after the end of treatment.

2. Materials and methods

2.1. Animal husbandry

Ten-week-old male C57BL/6 (n = 234) and BALB/c (n = 130) mice (Envigo Srl, Udine, Italy) were employed for this study. The experimental procedure were performed in agreement with national (D. L.vo 26/2014, Gazzetta Ufficiale della Repubblica Italiana, n.61, March 14th 2014) and international laws and policies (European Union directive 2010/63/UE; Guide for the Care and Use of Laboratory Animals, U.S. National Research Council, 1996). Approval for the study was obtained from the Italian Ministry of Health (n. 919/2015-PR).

Animals were maintained under standard animal housing conditions, thus with a 12 h light–dark cycle and a room temperature and relative humidity at 20 ± 2 °C and 55 ± 10%, respectively. Drug- and vehicle-treated mice were housed separately with free access to water and food. During the neurophysiological recording, mice were anesthetized with isoflurane and their body temperature was maintained constant using a heating pad. At each experimental time point mice were sacrificed and tissue samples collected.

2.2. Drug

Oxaliplatin (OHP) 5 mg/ml concentrate for infusion (Accord Healthcare Limited, UK) was diluted in 5% glucose solution to achieve the desired concentration immediately before each administration.

Using injection volume of 10 ml/kg, mice were treated intraperitoneally (i.p.) or intravenously (i.v.) with different concentrations of oxaliplatin (OHP groups) or 5% glucose solution as vehicle (CTRL groups), as reported in Table 1.

The OHP schedules of treatment reproduced in this study were previously published by Nassini et al., Andoh, Gauchan, Sakamoto workgroups (*Study 1*) (Andoh et al., 2019; Andoh et al., 2016; Andoh et al., 2015; Andoh et al., 2013; Gauchan et al., 2009a, 2009c; Nassini et al., 2011; Sakamoto et al., 2016); Jiang et al. (*Study 2*) (Jiang et al., 2016); Ta, Coriat workgroups (*Study 3*) (Coriat et al., 2014; Ta et al., 2009); Renn et al., Marmiroli et al. with dosage adjustment (*Study 4*) (Marmiroli et al., 2017a; Renn et al., 2011).

2.3. Experimental design

Four models with very different oxaliplatin doses, type of injection and treatment schedules (short or long-term treatment) were reproduced in our laboratories.

For each study, mice were randomly divided in two groups of 13 mice for each group/time point, i.e. an OHP group treated with one of the four different schedules and their corresponding vehicle groups (*Studies 1–4*). In order to verify the OIPN onset, we used a multimodal analysis approach at different time points (d1 represents the first day of drug administration). Hence, at each experimental time point 26 mice (n = 13/group) were subjected to behavioural tests (Dynamic and Cold Plate tests) and neurophysiological examination. The day after the in vivo evaluations, 26 mice/time point (n = 13/group) from the original cohort were sacrificed for biological sampling: L4-L5 dorsal root ganglia (DRG), caudal and sciatic nerves were collected for morphological and morphometric analyses and skin biopsy was processed for the evaluation of intraepidermal nerve fibres (IENF) density.

The summary of experimental design of the study is represented in Table 1.

2.4. OIPN assessment

2.4.1. Clinical monitoring and body weight

The mortality and general condition of the animals were evaluated daily. Body weight was recorded before each OHP injection for general toxicity assessment and for drug dose adjustment, and weekly during follow-up period to monitor animal health.

2.4.2. Behavioural assessment

In order to evaluate mechanical and thermal (cold) sensitivity, at each experimental time point withdrawal thresholds of 26 mice (n = 13/ group) were determined by Dynamic test and Cold Plate test respectively. The *mechanical threshold* was assessed using Dynamic Aesthesiometer apparatus (model 37,450 - Dynamic Plantar Aesthesiometer, Ugo Basile Biological Instruments, Comerio, Italy). Before testing, each animal was placed in the device Plexiglas chamber for a 2-h acclimatization period. A pointed metallic filament with 0.5 mm diameter, which exerted a progressively increasing pressure reaching up to 15 g within 15 s, was applied to the plantar surface of the hind paw. Paw withdrawal latencies were recorded three times for each hind paw and the average of the results represented the mechanical threshold expressed in grams. In order to avoid skin damage the cut-off was set at 15 s, after which the mechanical stimulus was automatically stopped. The *cold nociceptive threshold* was assessed using the Cold Plate apparatus (model 35,100 - Hot/Cold Plate, Ugo Basile Biological Instruments, Comerio, Italy). This device is composed by a Plexiglass cylinder and a thermostatic plate set at +4 °C. During the test, each mouse was placed in the Plexiglass holding cage, free to move and walk. The number of pain signs/suffering (hind paws lifts, flicking/licking and jumping) were recorded in a trial of 5 min. The trial was prematurely suspended if the animal showed signs of a strong sensitivity to temperature (evident anxiety and vocalization) (Marmiroli et al., 2017a).

2.4.3. Neurophysiological evaluation

Neurophysiological assessment was determined in caudal and digital nerves using an electromyography apparatus (Myto2 ABN Neuro, Firenze, Italy). Briefly, Nerve Conduction Velocity (NCV) and Sensory Nerve Action Potential (SNAP) amplitude were measured by placing a couple of needle recording electrodes (cathode and anode) at the base of the tail (for caudal recordings) or at the ankle bone (for digital recordings) and a couple of stimulating electrodes 3.5 cm far from the recording points (for caudal recordings) or close to the fourth toe (for

Table 1
The table summarizes the OHP schedules of treatment reproduced and the evaluation time points considered for each study.*

	Strain	Animals/group	OHP dose	Treatment schedule	Cumulative dose	Weekly dose intensity	Evaluation time points
Study 1	C57BL/6	39	3 mg/kg	single i.p.	3 mg/kg	3 mg/kg	d2 (24h from the dose) d8 (1 wk. FU) d15 (2 wk. FU)
Study 2	C57BL/6	39	10 mg/kg	i.p. injection at d1 and d3	20 mg/kg	20 mg/kg	d4 (24h after the 2nd dose) d10 (1 wk. FU) d17 (2 wk. FU)
Study 3	C57BL/6	39	3 mg/kg	i.p daily injection, 2 cycles at d1–5 and d11–15	30 mg/kg	15 mg/kg	d8 (3d after the end of 1st cycle) d18 (3d after the end of 2nd cycle) d29 (2 wk. FU)
Study 4	BALB/c	65	5 mg/kg	i.v. injection, 2qwx4	40 mg/kg	10 mg/kg	d2 (24h from the first dose) d8, d15, d30 (5d after the last dose) d39 (2 wk. FU)

i.p./i.v. = intraperitoneal or intravenous administration, d = day of the study, h = hours, wk. = week, FU = follow-up.
* CTRL groups: treatment with glucose solution 5% for each study, following the relative OHP schedule.

digital recordings). Latencies were measured from stimulus onset and peak-to-peak amplitudes were calculated. The NCV was calculated considering the measured distance between the recording and the stimulating points divided by the latency from the stimulus artefact to the onset of the first peak of the elicited action potential (Marmiroli et al., 2017a; Renn et al., 2011).

2.4.4. Morphological and morphometric evaluation

Pathological assessments were performed on L4-L5 DRG, caudal and sciatic nerves and hind paw skin biopsies collected from 6 randomly selected mice (n = 3/group) at each experimental time point. Briefly, DRG and nerves were immediately fixed in 2% glutaraldehyde/4% paraformaldehyde and 3% glutaraldehyde, respectively, in 0.12 M phosphate buffer solutions pH 7.4. Samples were then post-fixed in OsO_4 and embedded in epoxy resin. Serial 1.5-μm sections were prepared, stained with toluidine blue and examined with a Nikon Eclipse E200 light microscope (Leica Microsystems GmbH, Wetzlar, Germany) for morphological observations. Images of DRG and nerves were captured with a light microscope-incorporated camera at a magnification of 20× and 60× respectively by QWin software (Leica DFC 280, Wetzlar, Germany) to perform morphometric analyses. The somatic, nuclear and nucleolar areas of at least 200 DRG neurons/animal were manually measured with an image analyser (Image J software, US National Institutes of Health). The mean diameter, frequency distribution and density of myelinated fibres were calculated using an automatic image analyser (Image-Pro Plus compiled by Immagini e Computer SNC, Milan, Italy). Biopsies of the plantar hind paw skin were immediately fixed in PLP 2% (paraformaldehyde-lysine-sodium periodate) solution and freezed. Then, 20-μm-thick cryostat sections were immunostained with rabbit polyclonal anti-protein gene product 9.5 (PGP 9.5; GeneTex, Irvine, CA) using a free-floating protocol. The total number of PGP 9.5-positive IENF crossing the dermal-epidermal junction was counted under a light microscope at 40× magnification (Nikon Eclipse E200 light microscope, Leica Microsystems GmbH, Wetzlar, Germany) and divided by the length in mm of derma (Marmiroli et al., 2017a; Renn et al., 2011).

2.5. Statistical analysis

At the established time points, the differences between two groups (OHP-treated vs CTRL mice) were statistically analysed by unpaired t-test for body weight and morphometric evaluations and by Mann-Whitney nonparametric test for behavioural, neurophysiological recordings and IENF density (GraphPad Prism Software Inc., San Diego, CA). A difference was considered significant if $p < .05$. Data are reported in Tables 2–5 as means and standard deviations (SD). Supplemental data, Table S6–S9, show medians and interquartile ranges (25% Percentile-75% Percentile) of the data reported in Tables 2–5 included in the text.

3. Results

3.1. Study 1

OHP 3 mg/kg single i.p. administration in C57BL/6 mice.

3.1.1. Clinical monitoring and body weight

No mortality, deterioration of health status or significant changes in body weight were observed in treated mice compared to CTRL group (Supplementary material Fig. S1A).

3.1.2. Behavioural assessment

No significant changes in mechanical and cold withdrawal thresholds were observed in OHP-treated mice compared to CTRL for the entire period of observation (d2, d8 and d15). Despite the limited interval between each determination no learning effect was observed with the automated systems used in these studies (Table 2, Supplementary material Table S6).

3.1.3. Neurophysiological evaluation

No alterations in SNAP amplitude and NCV recorded in caudal and digital nerves of OHP-treated mice were observed at d2, d8 and d15 (Table 2, Supplementary material Table S6).

3.1.4. Morphological and morphometric evaluation

At the pathological examination, DRG and peripheral nerves did not show evident morphological alterations at d8 and d15 after drug delivery. Morphometric assessment of caudal and sciatic nerves and IENF density evaluation were performed at d8 after OHP administration and did not show any significant difference between treated and control mice. A significant decrease in nuclear size was observed in DRG of OHP-treated mice sacrificed at d8 ($p < .0001$) but returned to normal values at d15 (Table 2, Supplementary material Fig. S2 and Table S6).

3.2. Study 2

OHP 10 mg/kg, two i.p. administration at d1 and d3 in C57BL/6 mice.

3.2.1. Clinical monitoring and body weight

All mice survived until the end of the study and a normal general health status of the animals was observed. In this model, the body weight of OHP-injected animals decreased after the first administration and during the entire period of observation, becoming significant at d10

Table 2
Behavioural, neurophysiological and neuropathological changes in OHP-treated mice and CTRL of *Study 1*.****

	(^)	d2	d8	d15
Behavioural assessment				
Mechanical withdrawal threshold (gr)	CTRL	5.33 (0.46)	5.18 (0.33)	5.52 (0.63)
	OHP	5.33 (0.33)	5.35 (0.25)	5.34 (0.42)
Cold withdrawal threshold (n° of signs)	CTRL	17.85 (6.05)	15.08 (5.78)	20.69 (7.45)
	OHP	18.38 (6.18)	15.46 (3.68)	23.77 (5.77)
Neurophysiology				
Caudal SNAP (μV)	CTRL	123.5 (24.28)	113.1 (19.53)	124.9 (26.33)
	OHP	117.6 (26.17)	108.2 (14.34)	119.8 (25.79)
Caudal NCV (m/s)	CTRL	33.44 (1.00)	33.25 (1.27)	32.64 (1.62)
	OHP	32.98 (1.24)	33.38 (0.90)	33.38 (1.37)
Digital SNAP (μV)	CTRL	120.9 (39.26)	108.7 (26.00)	109.0 (23.33)
	OHP	123.6 (32.44)	116.1 (15.74)	105.1 (20.01)
Digital NCV (m/S)	CTRL	29.84 (1.85)	29.26 (1.89)	28.77 (0.99)
	OHP	29.70 (1.58)	29.30 (1.92)	29.25 (1.74)
DRG morphometry				
Somatic area (μm^2)	CTRL	//	561.6 (343.4)	552.9 (340.3)
	OHP	//	529.5 (336.7)	522.8 (343.1)
Nuclear area (μm^2)	CTRL	//	97.14 (47.56)	96.13 (47.10)
	OHP	//	84.02 (37.66)****	93.23 (47.27)
Nucleolar area (μm^2)	CTRL	//	6.77 (4.41)	6.62 (4.30)
	OHP	//	6.39 (4.33)	6.34 (4.37)
Nerve morphometry				
Sciatic nerve fibre diameter (μm)	CTRL	//	5.01 (1.66)	//
	OHP	//	5.04 (1.63)	//
Caudal nerve fibre diameter (μm)	CTRL	//	5.25 (1.19)	//
	OHP	//	5.22 (1.22)	//
Epidermal nerve fibres morphometry				
IENF density (fibres/mm)	CTRL	//	30.80 (1.35)	//
	OHP	//	30.86 (2.51)	//

Mean values and standard deviations (SD). ****p < .0001 vs CTRL, Unpaired t-test. // = not determined; (^) = sampling was performed the day after behavioural and neurophysiological assessment.

Table 3
Behavioural, neurophysiological and neuropathological changes in OHP-treated mice and CTRL of *Study 2*.

	(^)	d4	d10	d17
Behavioural assessment				
Mechanical withdrawal threshold (gr)	CTRL	5.72 (0.58)	5.73 (0.81)	5.82 (0.46)
	OHP	5.90 (0.37)	5.72 (0.81)	5.66 (0.54)
Cold withdrawal threshold (n° of signs)	CTRL	18.38 (6.82)	17.54 (8.16)	17.00 (4.43)
	OHP	19.00 (6.70)	25.46 (6.46)**	25.46 (9.02)*
Neurophysiology				
Caudal SNAP (μV)	CTRL	145.5 (15.29)	142.4 (25.68)	145.4 (18.44)
	OHP	133.4 (41.64)	125.9 (31.06)	134.5 (33.40)
Caudal NCV (m/s)	CTRL	30.68 (2.20)	33.04 (1.69)	31.95 (2.12)
	OHP	31.71 2.60)	31.75 (2.67)	33.30 (1.18)
Digital SNAP (μV)	CTRL	101.9 (32.28)	151.8 (61.18)	116.4 (50.11)
	OHP	123.8 (34.01)	115.9 (35.51)	122.9 (38.52)
Digital NCV (m/S)	CTRL	32.08 (1.97)	32.68 (2.34)	31.83 (2.96)
	OHP	31.49 (1.93)	33.38 (2.85)	34.20 (3.16)
DRG morphometry				
Somatic area (μm^2)	CTRL	//	522.9 (344.4)	564.4 (370.3)
	OHP	//	454.5 (305.2)***	475.5 (290.9)****
Nuclear area (μm^2)	CTRL	//	94.02 (49.79)	99.74 (47.13)
	OHP	//	85.42 (45.02)**	88.62 (51.46)***
Nucleolar area (μm^2)	CTRL	//	6.35 (3.93)	5.94 (3.98)
	OHP	//	5.57 (3.18)****	5.70 (3.08)
Nerve morphometry				
Sciatic nerve fibre diameter (μm)	CTRL	//	5.73 (1.98)	5.50 (1.92)
	OHP	//	5.30 (1.87)****	5.40 (1.98)
Caudal nerve fibre diameter (μm)	CTRL	//	5.27 (1.38)	4.98 (1.45)
	OHP	//	5.01 (1.36)****	4.92 (1.40)
Epidermal nerve fibres morphometry				
IENF density (fibres/mm)	CTRL	//	30.74 (4.19)	31.95 (2.93)
	OHP	//	29.41 (2.23)	31.16 (4.04)

Mean values and standard deviations (SD). *p < .05, **p < .01, ***p < .001, ****p < .0001 vs CTRL, Unpaired t-test or Mann-Whitney nonparametric test. // = not determined; (^) = sampling was performed the day after behavioural and neurophysiological assessment.

Table 4
Behavioural, neurophysiological and neuropathological changes in OHP-treated mice and CTRL of *Study 3*.

	(^)	d8	d18	d29
Behavioural assessment				
Mechanical withdrawal threshold (gr)	CTRL	5.39 (0.53)	5.33 (0.43)	5.37 (0.44)
	OHP	5.54 (0.43)	5.55 (0.44)	5.14 (0.38)
Cold withdrawal threshold (n° of signs)	CTRL	14.38 (4.53)	16.15 (3.55)	14.00 (3.65)
	OHP	19.00 (7.08)	12.15 (4.16)*	10.69 (3.32)*
Neurophysiology				
Caudal SNAP (μV)	CTRL	120.8 (22.31)	144.7 (22.56)	124.3 (24.01)
	OHP	117.2 (22.37)	144.8 (30.66)	122.4 (17.95)
Caudal NCV (m/s)	CTRL	32.54 (1.58)	33.10 (1.12)	33.25 (1.55)
	OHP	32.95 (2.00)	33.04 (1.34)	33.45 (0.85)
Digital SNAP (μV)	CTRL	116.6 (25.75)	127.2 (25.54)	117.8 (30.80)
	OHP	121.2 (33.84)	117.9 (29.43)	127.1 (20.64)
Digital NCV (m/S)	CTRL	28.50 (1.56)	27.86 (1.18)	28.18 (1.53)
	OHP	29.22 (1.65)	27.84 (1.61)	27.79 (1.06)
DRG morphometry				
Somatic area (μm^2)	CTRL	595.8 (388.6)	527.6 (341.7)	582.9 (363.9)
	OHP	494.0 (331.5)****	482.9 (309.3)*	500.5 (349.1)****
Nuclear area (μm^2)	CTRL	93.58 (44.34)	87.98 (43.94)	102.20 (49.67)
	OHP	88.75 (41.69)	82.42 (37.26)*	94.10 (52.16)**
Nucleolar area (μm^2)	CTRL	6.37 (4.09)	6.19 (4.14)	6.47 (4.09)
	OHP	5.15 (3.16)****	5.05 (2.72)****	5.13 (2.88)****
Nerve morphometry				
Sciatic nerve fibre diameter (μm)	CTRL	//	5.64 (2.01)	5.28 (1.74)
	OHP	//	5.75 (1.93)	5.19 (1.73)
Caudal nerve fibre diameter (μm)	CTRL	//	5.08 (1.40)	5.33 (1.31)
	OHP	//	5.22 (1.37)**	5.31 (1.27)
Epidermal nerve fibres morphometry				
IENF density (fibres/mm)	CTRL	//	28.28 (2.66)	32.18 (3.36)
	OHP	//	29.10 (4.20)	31.86 (2.42)

Mean values and standard deviations (SD). *p < .05, **p < .01, ****p < .0001 vs CTRL, Unpaired t-test or Mann-Whitney nonparametric test. // = not determined; (^) = sampling was performed the day after behavioural and neurophysiological assessment.

Table 5
Behavioural, neurophysiological and neuropathological changes in OHP-treated mice and CTRL of *Study 4*.

	(^)	d2	d8	d15	d30	d39
Behavioural assessment						
Mechanical withdrawal threshold (gr)	CTRL	5.48 (0.49)	5.39 (0.51)	5.24 (0.37)	5.50 (0.42)	5.37 (0.30)
	OHP	5.60 (0.43)	5.18 (0.35)	5.27 (0.46)	4.86 (0.25)***	4.94 (0.45)*
Cold withdrawal threshold (n° of signs)	CTRL	10.46 (2.10)	16.15 (5.33)	14.42 (3.39)	17.46 (3.97)	13.85 (5.09)
	OHP	21.31 (9.62)****	23.77 (10.60)	22.54 (5.84)**	24.31 (8.55)*	17.38 (3.82)
Neurophysiology						
Caudal SNAP (μV)	CTRL	118.1 (23.05)	122.0 (19.32)	126.4 (16.99)	116.0 (16.73)	85.02 (23.06)
	OHP	123.7 (21.56)	107.4 (28.73)	104.5 (13.59)**	89.62 (19.91)**	108.1 (22.36)
Caudal NCV (m/s)	CTRL	34.03 (0.76)	31.88 (1.13)	33.49 (0.83)	37.44 (1.04)	32.94 (1.30)
	OHP	33.62 (0.66)	32.75 (1.14)	33.28 (0.52)	36.73 (1.44)	33.78 (0.78)
Digital SNAP (μV)	CTRL	103.5 (18.75)	90.51 (15.90)	82.47 (14.52)	131.4 (27.79)	95.31 (22.06)
	OHP	100.5 (19.98)	82.05 (20.89)	81.55 (17.07)	92.44 (20.80)****	88.21 (25.33)
Digital NCV (m/S)	CTRL	28.28 (1.66)	28.02 (1.13)	27.55 (1.31)	28.08 (1.65)	28.23 (0.76)
	OHP	28.94 (1.54)	27.70 (1.42)	27.20 (1.15)	27.52 (1.45)	28.15 (1.26)
DRG morphometry						
Somatic area (μm^2)	CTRL	//	505.2 (344.7)	540.5 (331.8)	483.0 (298.9)	505.2 (344.7)
	OHP	//	525.8 (332.5)	596.5 (353.1)**	445.0 (299.3)*	483.5 (317.9)
Nuclear area (μm^2)	CTRL	//	89.25 (44.25)	95.36 (47.72)	88.12 (41.39)	89.25 (44.25)
	OHP	//	91.33 (42.46)	103.2 (48.80)**	78.9 (38.92)****	86.95 (44.55)
Nucleolar area (μm^2)	CTRL	//	7.18 (4.59)	7.74 (4.75)	6.56 (4.16)	7.18 (4.59)
	OHP	//	6.81 (4.29)	7.45 (4.55)	6.14 (3.58)	6.77 (4.06)
Nerve morphometry						
Sciatic nerve fibre diameter (μm)	CTRL	//	//	5.77 (1.89)	6.49 (2.08)	5.99 (2.05)
	OHP	//	//	5.76 (1.88)	6.01 (1.99)****	5.79 (1.82)**
Caudal nerve fibre diameter (μm)	CTRL	//	//	5.13 (1.35)	5.40 (1.48)	5.15 (1.41)
	OHP	//	//	5.13 (1.42)	5.05 (1.35)****	5.19 (1.50)
Epidermal nerve fibres morphometry						
IENF density (fibres/mm)	CTRL	//	//	//	29.26 (2.04)	30.05 (2.88)
	OHP	//	//	//	19.95 (2.68)****	22.60 (2.13)****

Mean values and standard deviations (SD). *p < .05, **p < .01, ***p < .001, ****p < .0001 vs CTRL, Unpaired t-test or Mann-Whitney nonparametric test. // = not determined; (^) = sampling was performed the day after behavioural and neurophysiological assessment.

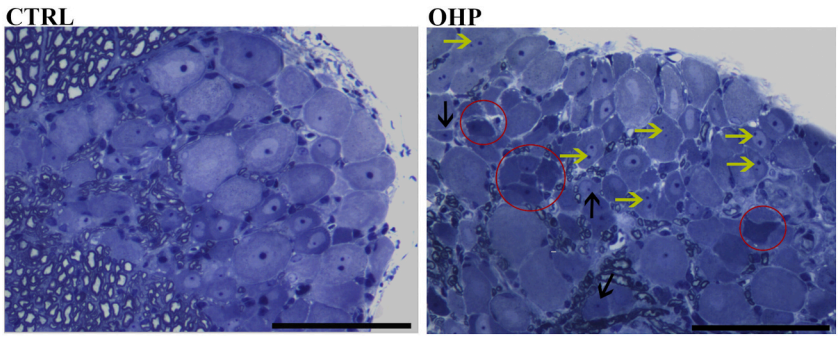

Fig. 1. Morphology of DRG neurons at d30 of *Study 4*. (For interpretation of the references to color in this figure legend, the reader is referred to the web version of this article.)
At the end of treatment (d30^), OHP induced neuron degeneration (circles), multiple (yellow arrows) and eccentric (black arrows) nucleoli in DRG.
20x magnification. Scale bar 100 μm.
(^) = sampling was performed the day after behavioural and neurophysiological assessment.

(p < .01) (Supplementary material Fig. S1B).

3.2.2. Behavioural assessment

Cold hyperalgesia was observed in OHP-treated mice at d10 (p < .01) and d17 (p < .05). The treatment did not induce significant changes in mechanical withdrawal threshold (Table 3, Supplementary material Table S7).

3.2.3. Neurophysiological evaluation

The OHP-treated mice did not show any significant difference in SNAP amplitude and NCV measured in caudal and digital nerves, compared to CTRL mice at d4, d10 and d17 (Table 3, Supplementary material Table S7).

3.2.4. Morphological and morphometric evaluation

Light microscopy analysis did not evidence apparent morphological changes in DRG neurons and peripheral nerves of OHP-treated mice. DRG morphometric assessment showed a significant decrease in the size of cell body (p < .001), nucleus (p < .01) and nucleolus (p < .0001) in OHP-treated animals compared to CTRL at d10. The reduction of somatic (p < .0001) and nuclear (p < .001) areas persisted at d17, whereas the nucleolar area returned to a normal value. This treatment also induced a significant reduction of the mean diameter of myelinated fibres in sciatic and caudal nerves at d10 (p < .0001), that returned to normal at d17. IENF density did not change in OHP group compared to CTRL one at 1 week (d10) and 2 weeks (d17) of follow-up (Table 3, Supplementary material Fig. S3 and Table S7).

3.3. Study 3

OHP 3 mg/kg, i.p., daily, two cycles at d1–5 and d11–15 in C57BL/6 mice.

3.3.1. Clinical monitoring and body weight

We observed no mortality and no severe general toxicity of OHP-treated mice compared to CTRL even though there was a significant decrease in the body weight after the 3rd OHP injection of the first 5-day cycle (d8; p < .01). Such decline progressed after the second cycle of treatment (d18; p < .001) and remained significant for the entire 30-day period of observation (d29; p < .01) (Supplementary material, Fig. S1C).

3.3.2. Behavioural assessment

OHP treatment did not induce significant changes in mechanical withdrawal thresholds. Non-significant trend toward cold hyperalgesia was observed at the examination performed after the first cycle (d8), whereas in the subsequent examination performed after the second cycle (d18) cold hypoalgesia was observed in OHP-treated mice and persisted after 2 weeks of follow-up (d29; p < .05) (Table 4, Supplementary material Table S8).

3.3.3. Neurophysiological evaluation

The treatment schedule did not induce any significant changes in SNAP amplitude and NCV recorded in caudal and digital nerves at d8, d18 and d29 (Table 4, Supplementary material Table S8).

3.3.4. Morphological and morphometric evaluation

Pathological examinations of DRG neurons and peripheral nerves did not show any relevant changes following OHP treatment. However, morphometric assessment evidenced significant reduction of somatic (p < .0001) and nucleolar (p < .0001) areas of DRG neurons as early as after the first OHP cycle of treatment (d8). This reduction persisted in cell body (p < .05; p < .0001), nucleus (p < .05; p < .01) and nucleolus (p < .0001; p < .0001) at the end of the second cycle (d18) and also at 2 weeks of follow-up (d29). Morphometric analysis revealed no significant difference of the mean diameters, densities and distribution of myelinated fibres in sciatic nerves. However, a mild difference in the mean diameter of myelinated fibre was observed in caudal nerves in OHP-treated mice compared to CTRL at d8 (p < .001). This difference was not confirmed at the subsequent examination performed after the second cycle of OHP (d18). The IENF density did not change in OHP-treated mice compared to CTRL group after the two cycles of OHP treatment (d18) and at 2 weeks of follow-up (d29) (Table 4, Supplementary material Fig. S4 and Table S8).

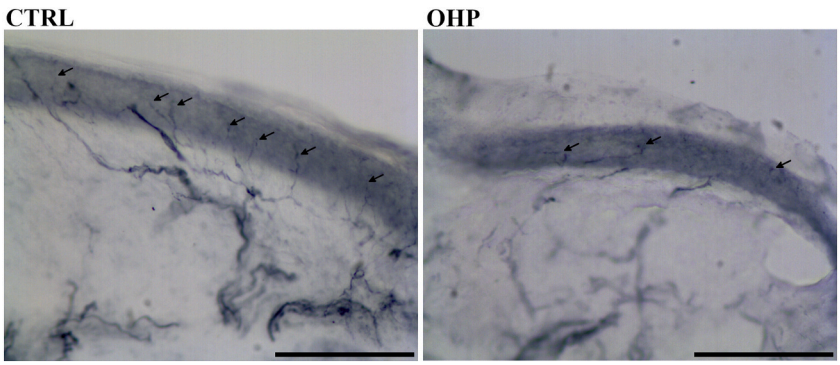

Fig. 2. Hind paw skin biopsies at d30 of *Study 4*. (For interpretation of the references to color in this figure legend, the reader is referred to the web version of this article.)
At the end of treatment (d30^), OHP induced a reduction of IENF (arrows) density in the hind paw skin biopsies.
20x magnification. Scale bar 100 μm.
(^) = sampling was performed the day after behavioural and neurophysiological assessment.

3.4. Study 4

OHP 5 mg/kg, i.v., twice weekly for 4 weeks in BALB/c mice.

3.4.1. Clinical monitoring and body weight

All OHP-treated mice survived until the end of the study and no deterioration in general health status was observed. However, approximately 20% of them developed piloerection and mild kyphosis together with a significant body weight loss compared to their CTRL from the last injection (d30; $p < .05$) up to the end of the study (d39; $p < .001$) (Supplementary material Fig. S1D).

3.4.2. Behavioural assessment

Compared to CTRL, mice treated with OHP for 4 weeks (d30; $p < .001$) developed mechanical allodynia lasting until 2 weeks of follow-up (d39; $p < .05$). In addition, treated animals developed cold hyperalgesia as early as after 24 h from the first administration (d2; $p < .0001$) that was confirmed at d15 ($p < .001$) and also at d30 ($p < .05$), whereas it resolved after 2 weeks of follow-up (d39) (Table 5, Supplementary material Table S9).

3.4.3. Neurophysiological evaluation

Until d8 of OHP treatment no significant change in neurophysiological parameters was recorded in caudal and digital nerves. However, a significant reduction in SNAP amplitude of OHP-treated mice compared to CTRL was observed in caudal nerve after 2 weeks of treatment (d15; $p < .01$) and also in the digital nerve at the end of treatment (d30; $p < .0001$). Otherwise, NCV in the two nerves examined did not significantly differ in OHP-treated mice compared to CTRL at each evaluation time point (Table 5, Supplementary material Table S9).

3.4.4. Morphological and morphometric evaluation

Regarding DRG morphology, at the end of treatment (d30) DRG neurons of OHP-treated mice showed some degenerating neurons and multiple and eccentric nucleoli (Fig. 1). In addition, OHP treatment induced alterations in neuronal size at d15 and d30. In particular, somatic ($p < .01$) and nuclear ($p < .01$) areas showed a significant increase at mid-treatment (d15), whereas a significant reduction in the area of the same neuronal structures (soma $p < .05$, nucleus $p < .0001$) was detected at the end of treatment (d30). DRG neuronal size of animals injected with OHP returned comparable to the values observed in CTRL group at 2 weeks of follow-up (d39). Regarding peripheral nerves, a significant decrease in the mean diameter of myelinated fibres was observed in sciatic nerve of OHP-treated mice at d30 ($p < .0001$) and d39 ($p < .01$). The fibre density distribution curve shows a shift to the left in sciatic nerves of OHP-treated mice compared to CTRL at each time point, slightly less evident at d15, indicating a trend in losing fibres of large calibre. A significant decrease in the mean diameter of myelinated fibres was also observed in caudal nerve at the end of treatment (d30; $p < .0001$). Moreover, at this evaluation time point a significant reduction in IENF density was also observed at light microscopy analysis of the hind paw skin biopsies of OHP-treated mice compared to CTRL group (Fig. 2, $p < .0001$). The reduction of the small unmyelinated fibres persisted after 2 weeks of follow-up period (d39; $p < .0001$) (Table 5, Supplementary material Fig. S5 and Table S9).

4. Discussion

Experimental animal models of human diseases are widely used to increase knowledge on the underlying pathophysiology and to test new treatments. One of the main concerns in their use is the translation of the preclinical findings into clinical practice, that is not always easy and reliable. This is partly due to unavoidable differences among species, but also because in some cases the animal model of a disease does not closely reproduce the complexity of human pathology, and they lack information in terms of pathological characterization.

In the field of peripheral neuropathies, the availability of reliable experimental animal models of CIPN, able to mimic the clinical features, is an useful tool to understand the molecular mechanisms of this still untreatable pathology and to identify targets able to prevent it or to limit its severity (Cavaletti and Marmiroli, 2020). OIPN is extensively studied at preclinical level because OHP is an effective and widely used chemotherapeutic drug, but it is severely neurotoxic, with a combined acute and chronic pattern. Cold-triggered paresthesias and dysesthesias at the extremities and at the oropharyngolaryngeal region are common adverse effects associated with acute OHP administration while a distal length-dependent axonal neuropathy can develop after repeated administrations and may persist/worsen after the discontinuation of the therapy up to six months or even after years ("coasting" phenomenon) (Avan et al., 2015; Cavaletti and Marmiroli, 2015; Velasco and Bruna, 2010; Zajaczkowska, et al., 2019).

In order to characterize the complex physiological events underlying this neurological complication, many different rodent models of OIPN have been described (Calls et al., 2020; Gadgil et al., 2019). Most of them have been evaluated with behavioural methods, but not investigated also at neurophysiological and pathological levels. Neurotoxicity assessment merely based on behavioural tests as outcome measures, without verifying the presence and extent of peripheral nervous system (PNS) damage with additional, complementary methods, could potentially evidence only part of the OHP-related effects, namely neuropathic pain. Besides neurophysiological evaluation (the gold standard for the diagnosis of neuropathy in clinical practice) and behavioural tests, only a detailed morphological and morphometric examination of DRG, peripheral nerves and skin biopsies allow to provide firm and direct evidence of the pathological changes induced by OHP treatment, and to verify whether they are comparable with the effects obtained by OHP administration in clinical practice.

Previous experimental studies about OHP neurotoxicity demonstrated that DRG neurons are the drug main target, with secondary axonal changes (Avan et al., 2015; Cavaletti et al., 2001; Kanat et al., 2017). Accordingly, in human OIPN the pathological hallmarks are related to axonopathy, clinically demonstrated not only as reduction of the SNAP amplitude at the neurophysiological examination, but also as reduction in IENF density at the skin biopsy as well as at the corneal level (Burakgazi et al., 2011; Campagnolo et al., 2013). Therefore, the presence of these features should be considered as a necessary requirement for any reliable animal model aiming at reproducing the full spectrum of OHP neurotoxicity.

This work aimed to make a direct comparison, including extensive pathological assessment, among four different OIPN mouse models selected from the published literature because of their very different single dose levels (3–10 mg/kg;), weekly dose intensities (3–20 mg/kg), treatment durations (1–28 days), ways of delivery (i.p. vs i.v.), and mouse strains (C57BL/6 vs BALB/c). These models were examined at similar intervals after drug delivery and with the same set of assessments performed by single examiners.

The results of our comparative analysis evidenced remarkable differences in the results obtained in the selected OIPN animal models. Examination performed after the single dose of OHP used in *Study 1*, did not show any change in neurophysiological and behavioural tests. Minimal pathological changes were observed only after extensive morphometric analysis of the DRG neurons at the nuclear level and at a single point of assessment, whereas no alterations were evidenced in the peripheral nerves or in the skin biopsy. Following the higher-intensity treatments adopted in *Studies 2* and *3,* besides altered cold sensitivity, the effects at pathological level in DRG and peripheral nerves were more evident, although no change was observed in skin biopsies and in neurophysiological investigation. In particular, the use of high-intensity, but short-term, administration used in *Study 2* induced the reduction of neuronal size at both points of assessment whereas in the peripheral nerves a strong effect was observed 8 days

after the last administration, but it was no longer evident one week later. DRG neuronal atrophy occurred also in *Study 3* at the end of each 5-day cycle of OHP treatment and persisted after 2 weeks of follow-up. Using the longer treatment schedule in which OHP was administered twice a week over 4 weeks (*Study 4*), pathological changes at all the sample sites starting from the middle stage of treatment were observed. These findings, together with alterations of mechanical and thermal thresholds and neurophysiological changes, are consistent with ongoing axonopathy. These pathological changes disappeared in the DRG neurons, but persisted in the peripheral nerves and in skin biopsy at the follow-up examination, a time course that has been associated with the "coasting phenomenon" typical of platinum-based drugs (Cavaletti et al., 2001; Cavaletti et al., 1994). On the other hand, the complete recovery in SNAP amplitude detected as early as after 2 weeks of follow-up associated with the acceptable general toxicity could indicate that this mouse model probably would require further increase in dose-intensity of OHP treatment to more closely mimic the clinical situation. In fact, the chronic pattern of patients suffering from OIPN is associated with neurophysiological alterations that may persist for months or even years after discontinuation of therapy (Briani et al., 2014; Park et al., 2011). On the other hand, cold hyperalgesia observed in *Studies 2, 3* and *4* reliably replicates the acute form of neurotoxicity induced by this drug.

It is possible that one of the reasons for the more severe OIPN observed in *Study 4* is the prolonged treatment, since the weekly dose intensity is lower than in *Studies 2* and *3*. However, it is also likely that a major determinant is the different OHP pharmacokinetics due to the way of delivery, since it is well know that i.v. administration (i.e. that used in clinical practice) is characterized by a higher systemic drug exposure than i.p. one at the same drug dose. For example, in rat plasma peak platinum concentration is 30-fold higher after i.v. compared to i.p. administration of OHP 5 mg/kg at 5 min, then it declines to 4-fold at 30 min and remains 2-fold higher at 60 and 90 min (Pestieau et al., 2001). It should be noted as well that different results in pain sensitivity can be associated to strain differences (Mogil, 2009; Smith et al., 2004). In particular, we showed that BALB/c are mice more susceptible to the neurotoxic effects of OHP compared to C57BL/6 when exposed at the same treatment (Marmiroli et al., 2017a), suggesting that genetic variability may influence CIPN severity. Differences in DRG neurons neurotoxicity between different rodent strains following cisplatin and bortezomib treatments were also observed in an in vitro study conducted by Podratz and colleagues (Podratz et al., 2016).

The behavioural results obtained in the present study reproduced only in part those previously reported by other authors. It is likely that these discrepancies are also due to methodological reasons since we used different detection devices, but it should be noted that slightly inconstant results were reported in different studies by the same authors as well, despite using the same OHP treatment schedule and behavioural investigation method for the detection (Andoh et al., 2019; Andoh et al., 2016; Andoh et al., 2015; Andoh et al., 2013; Gauchan et al., 2009b, 2009c; Sakamoto et al., 2016).

5. Conclusions

In conclusion, the overall comparison among the different OIPN mouse models makes clear the fundamental importance of a multimodal approach in the study of OIPN, where behavioural test results are validated by neurophysiological and neuropathological evaluation. Thus, it cannot be ruled out that certain rodent models based only on sensory threshold determination could be able to reproduce OHP-induced neuropathic pain, but there is no evidence that they are also able to mimic the full spectrum of the clinical aspects of chronic neurotoxicity.

Supplementary data to this article can be found online at https://doi.org/10.1016/j.expneurol.2020.113458.

Author contributions

All authors critically revised the article and approved the final version of the manuscript.

Funding

This work was supported by Associazione Italiana Ricerca sul Cancro (AIRC Progetto IG 2016Id.18631) and the Italian PRIN Grant (#2017ZFJCS3) (GC).

Funding sources had no involvement in the study.

Declaration of Competing Interest

Authors have no competing interests to declare.

Acknowledgments

The expert technical assistance of Mario Bossi is gratefully acknowledged.

References

Andoh, T., Sakamoto, A., Kuraishi, Y., 2013. Effects of xaliproden, a 5-HT1A agonist, on mechanical allodynia caused by chemotherapeutic agents in mice. Eur. J. Pharmacol. 721, 231–236. https://doi.org/10.1016/j.ejphar.2013.09.030.

Andoh, T., Kitamura, R., Kuraishi, Y., 2015. Milnacipran inhibits oxaliplatin-induced mechanical allodynia through spinal action in mice. Biol. Pharm. Bull. 38, 151–154. https://doi.org/10.1248/bpb.b14-00581.

Andoh, T., Sakamoto, A., Kuraishi, Y., 2016. 5-HT1A receptor agonists, xaliproden and tandospirone, inhibit the increase in the number of cutaneous mast cells involved in the exacerbation of mechanical allodynia in oxaliplatin-treated mice. J. Pharmacol. Sci. 131, 284–287. https://doi.org/10.1016/j.jphs.2016.07.008.

Andoh, T., Fukutomi, D., Uta, D., Kuraishi, Y., 2019. Prophylactic repetitive treatment with the herbal medicine Kei-kyoh-zoh-soh-oh-shin-bu-toh attenuates Oxaliplatin-induced mechanical allodynia by decreasing spinal astrocytes. Evid. Based Complement. Alternat. Med. 2019. https://doi.org/10.1155/2019/4029694.

Avan, Abolfazl, Postma, T.J., Ceresa, C., Avan, Amir, Cavaletti, G., Giovannetti, E., Peters, G.J., 2015. Platinum-induced neurotoxicity and preventive strategies: past, present, and future. Oncologist 20, 411–432. https://doi.org/10.1634/theoncologist.2014-0044.

Briani, C., Argyriou, A.A., Izquierdo, C., Velasco, R., Campagnolo, M., Alberti, P., Frigeni, B., Cacciavillani, M., Bergamo, F., Cortinovis, D., Cazzaniga, M., Bruna, J., Cavaletti, G., Kalofonos, H.P., 2014. Long-term course of oxaliplatin-induced polyneuropathy: a prospective 2-year follow-up study. J. Peripher. Nerv. Syst. 19, 299–306. https://doi.org/10.1111/jns.12097.

Bruna, J., Alberti, P., Calls-Cobos, A., Caillaud, M., Damaj, M.I., Navarro, X., 2020. Methods for in vivo studies in rodents of chemotherapy induced peripheral neuropathy. Exp. Neurol. https://doi.org/10.1016/j.expneurol.2019.113154.

Burakgazi, A.Z., Messersmith, W., Vaidya, D., Hauer, P., Hoke, A., Polydefkis, M., 2011. Longitudinal assessment of oxaliplatin-induced neuropathy. Neurology 77, 980–986. https://doi.org/10.1212/WNL.0b013e31822cfc59.

Calls, A., Carozzi, V., Navarro, X., Monza, L., Bruna, J., 2020. Pathogenesis of platinum-induced peripheral neurotoxicity: insights from preclinical studies. Exp. Neurol. https://doi.org/10.1016/j.expneurol.2019.113141.

Campagnolo, M., Lazzarini, D., Fregona, I., Cacciavillani, M., Bergamo, F., Parrozzani, R., Midena, E., Briani, C., 2013. Corneal confocal microscopy in patients with oxaliplatin-induced peripheral neuropathy. J. Peripher. Nerv. Syst. 18, 269–271. https://doi.org/10.1111/jns5.12036.

Cavaletti, G., Marmiroli, P., 2015. Chemotherapy-induced peripheral neurotoxicity. Curr. Opin. Neurol. https://doi.org/10.1097/WCO.0000000000000234.

Cavaletti, G., Marmiroli, P., 2020. Management of oxaliplatin-induced peripheral sensory neuropathy. Cancers (Basel) 12, 1370. https://doi.org/10.3390/cancers12061370.

Cavaletti, G., Tredici, G., Marmiroli, P., Fabbrica, D., Braga, M., 1994. Off-treatment course of cisplatin-induced dorsal root ganglia neuronopathy in rats. In Vivo 8, 313–316.

Cavaletti, G., Tredici, G., Petruccioli, M.G., Dondè, E., Tredici, P., Marmiroli, P., Minoia, C., Ronchi, A., Bayssas, M., Griffon Etienne, G., 2001. Effects of different schedules of oxaliplatin treatment on the peripheral nervous system of the rat. Eur. J. Cancer 37, 2457–2463. https://doi.org/10.1016/S0959-8049(01)00300-8.

Coriat, R., Alexandre, J., Nicco, C., Quinquis, L., Benoit, E., Chéreau, C., Lemaréchal, H., Mir, O., Borderie, D., Tréluyer, J.M., Weill, B., Coste, J., Goldwasser, F., Batteux, F., 2014. Treatment of oxaliplatin-induced peripheral neuropathy by intravenous mangafodipir. J. Clin. Invest. 124, 262–272. https://doi.org/10.1172/JCI68730.

Gadgil, S., Ergün, M., van den Heuvel, S.A., van der Wal, S.E., Scheffer, G.J., Hooijmans, C.R., 2019. A systematic summary and comparison of animal models for chemotherapy induced (peripheral) neuropathy (CIPN). PLoS One 14. https://doi.org/10.1371/journal.pone.0221787.

Gauchan, P., Andoh, T., Kato, A., Kuraishi, Y., 2009a. Involvement of increased expression of transient receptor potential melastatin 8 in oxaliplatin-induced cold allodynia in mice. Neurosci. Lett. 458, 93–95. https://doi.org/10.1016/j.neulet.2009.04.029.

Gauchan, P., Andoh, T., Kato, A., Kuraishi, Y., 2009b. Involvement of increased expression of transient receptor potential melastatin 8 in oxaliplatin-induced cold allodynia in mice. Neurosci. Lett. 458, 93–95. https://doi.org/10.1016/j.neulet.2009.04.029.

Gauchan, P., Andoh, T., Kato, A., Sasaki, A., Kuraishi, Y., 2009c. Effects of the prostaglandin ei analog limaprost on mechanical allodynia caused by chemotherapeutic agents in mice. J. Pharmacol. Sci. 109, 469–472. https://doi.org/10.1254/jphs.08325SC.

Jiang, S.P., Zhang, Z.D., Kang, L.M., Wang, Q.H., Zhang, L., Chen, H.P., 2016. Celecoxib reverts oxaliplatin-induced neuropathic pain through inhibiting PI3K/Akt2 pathway in the mouse dorsal root ganglion. Exp. Neurol. 275, 11–16. https://doi.org/10.1016/j.expneurol.2015.11.001.

Kanat, O., Ertas, H., Caner, B., 2017. Platinum-induced neurotoxicity: a review of possible mechanisms. World J. Clin. Oncol. 8, 329–335. https://doi.org/10.5306/wjco.v8.i4.329.

Marmiroli, P., Riva, B., Pozzi, E., Ballarini, E., Lim, D., Chiorazzi, A., Meregalli, C., Distasi, C., Renn, C.L., Semperboni, S., Morosi, L., Ruffinatti, F.A., Zucchetti, M., Dorsey, S.G., Cavaletti, G., Genazzani, A., Carozzi, V.A., 2017a. Susceptibility of different mouse strains to oxaliplatin peripheral neurotoxicity: phenotypic and genotypic insights. PLoS One 12. https://doi.org/10.1371/journal.pone.0186250.

Marmiroli, P., Scuteri, A., Cornblath, D.R., Cavaletti, G., 2017b. Pain in chemotherapy-induced peripheral neurotoxicity. J. Peripher. Nerv. Syst. 22, 156–161. https://doi.org/10.1111/jns.12226.

Mogil, J.S., 2009. Animal models of pain: progress and challenges. Nat. Rev. Neurosci. https://doi.org/10.1038/nrn2606.

Nassini, R., Gees, M., Harrison, S., De Siena, G., Materazzi, S., Moretto, N., Failli, P., Preti, D., Marchetti, N., Cavazzini, A., Mancini, F., Pedretti, P., Nilius, B., Patacchini, R., Geppetti, P., 2011. Oxaliplatin elicits mechanical and cold allodynia in rodents via TRPA1 receptor stimulation. Pain 152, 1621–1631. https://doi.org/10.1016/j.pain.2011.02.051.

Park, S.B., Lin, C.S.Y., Krishnan, A.V., Goldstein, D., Friedlander, M.L., Kiernan, M.C., 2011. Long-term neuropathy after oxaliplatin treatment: challenging the dictum of reversibility. Oncologist 16, 708–716. https://doi.org/10.1634/theoncologist.2010-0248.

Pestieau, S., Belliveau, J., Griffin, H., Stuart, O., Sugarbaker, P.H., 2001. Pharmacokinetics of intraperitoneal oxaliplatin: experimental studies. J. Surg. Oncol. 76. https://doi.org/10.1002/1096-9098(200102)76:2<106::AID-JSO1020>3.0.CO;2-E.

Podratz, J.L., Kulkarni, A., Pleticha, J., Kanwar, R., Beutler, A.S., Staff, N.P, Windebank, A.J., 2016. Neurotoxicity to DRG neurons varies between rodent strains treated with cisplatin and bortezomib. J. Neurol. Sci. 362, 131–135. https://doi.org/10.1016/j.jns.2015.12.038.

Renn, Cynthia L., Carozzi, V.A., Rhee, P., Gallop, D., Dorsey, S.G., Cavaletti, G., 2011. Multimodal assessment of painful peripheral neuropathy induced by chronic oxaliplatin-based chemotherapy in mice. Mol. Pain 7. https://doi.org/10.1186/1744-8069-7-29.

Sakamoto, A., Andoh, T., Kuraishi, Y., 2016. Involvement of mast cells and proteinase-activated receptor 2 in oxaliplatin-induced mechanical allodynia in mice. Pharmacol. Res. 105, 84–92. https://doi.org/10.1016/j.phrs.2016.01.008.

Smith, S.B., Crager, S.E., Mogil, J.S., 2004. Paclitaxel-induced neuropathic hypersensitivity in mice: responses in 10 inbred mouse strains. Life Sci. 74, 2593–2604. https://doi.org/10.1016/j.lfs.2004.01.002.

Ta, L.E., Low, P.A., Windebank, A.J., 2009. Mice with cisplatin and oxaliplatin-induced painful neuropathy develop distinct early responses to thermal stimuli. Mol. Pain 5https://doi.org/10.1186/1744-8069-5-9. 1744-8069-5-9.

Velasco, R., Bruna, J., 2010. Chemotherapy-induced peripheral neuropathy: an unresolved issue. Neurol. 25, 116–131. https://doi.org/10.1016/s2173-5808(10)70022-5. English Ed.

Vilholm, O.J., Christensen, A.A., Zedan, A.H., Itani, M., 2014. Drug-induced peripheral neuropathy. Basic Clin. Pharmacol. Toxicol. 115, 185–192. https://doi.org/10.1111/bcpt.12261.

Zajaczkowska, R., Kocot-Kępska, M., Leppert, W., Wrzosek, A., Mika, J., Wordliczek, J., 2019. Mechanisms of chemotherapy-induced peripheral neuropathy. Mol. Sci. Mech. Chemother. Peripher. Neuropathy. https://doi.org/10.3390/ijms200614515427.